

Supplementary Materials for

Tuning Dzyaloshinskii-Moriya Interaction via Electric Field at Co/h-BN Interface

C. Huang^{a,b,†}, L. Z. Jiang^{a,b,†}, Y. Zhu^{a,b,*}, Y. F. Pan^{a,b}, J. Y. Fan^{a,b}, C. L. Ma^c, J. Hu^{d,*} and D. N. Shi^{a,b,*}

^a Department of Physics, College of Science, Nanjing University of Aeronautics and Astronautics, Nanjing 210006, China

^b MIIT Key Laboratory of Aerospace Information Materials and Physics, Nanjing University of Aeronautics and Astronautics, Nanjing 211106, China

^c Jiangsu Key Laboratory of Micro and Nano Heat Fluid Flow Technology and Energy Application, School of Physical Science and Technology, Suzhou University of Science and Technology, Suzhou, 215009, China

^d China School of Physical Science and Technology, Ningbo University, Ningbo 315211, China

*) Electronic address: yzhu@nuaa.edu.cn (Y. Zhu); wlxmcl@mail.usts.edu.cn (C. L. Ma); hzhang@tmm.tu-darmstadt.de (H. B. Zhang)

†) These authors contributed equally to this work

S1. Adsorption positions

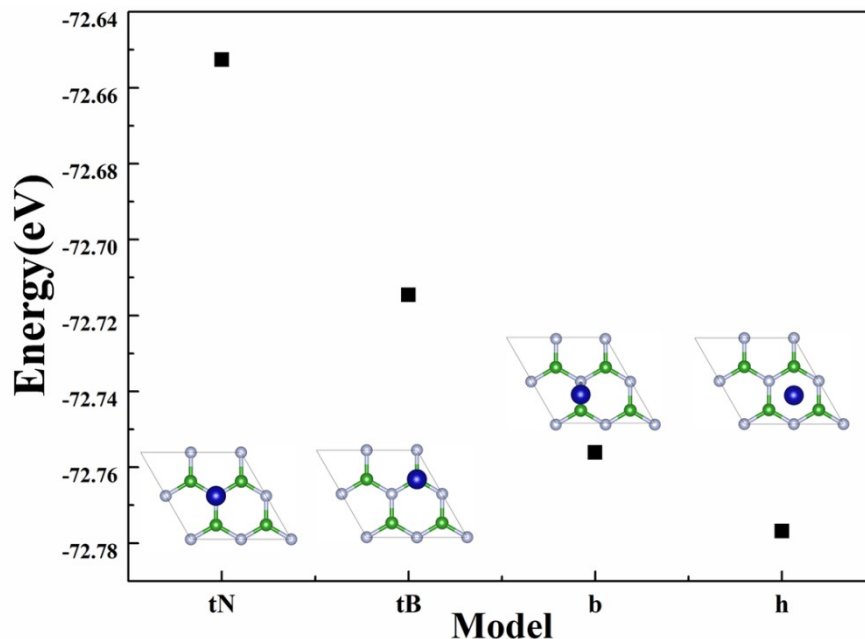


Fig. S1 (Color online) Energy of Co/h-BN interface as a function on different adsorption sites of Co.

The insert top view configurations are the different adsorbed modes.

Here, we compare the results for the variation of energy with different adsorbed structures.

The first one is the Co in the top position of the N (tN); the second is the Co in the top position of the B(tB); the third is the Co on the bridge site of the BN bond(b); the last is the Co in the hollow of h-BN hexagonal structure(h). As Fig. S1 shows, the h-site is the most stable adsorbed structure of all the calculated structures according to the energies. The optimized structural parameters for the obtained stable configurations are also presented in the table 2.

We fix the z coordinate of the Co atom and the farthest N atom, and then let the entire system relax, and get the graph between the energy and the z height. It is found that the

system has two bistable states, a higher position and a lower position under zero electric field and certain electric fields.

S2. Partial density of states

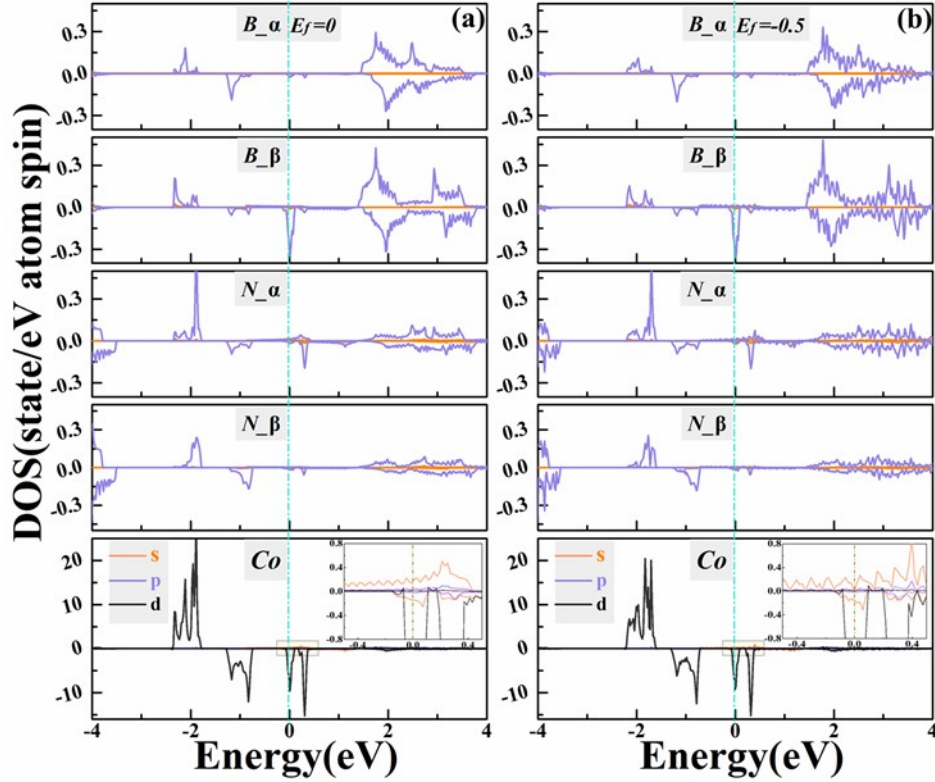


Fig. S2 (Color online) (a) and (b) Partial density of states (PDOS) for each atom of Co/h-BN in the electric field of -0.5 eV/\AA and 0 eV/\AA with SOC. The blue vertical dashed line denotes the Fermi level position.

As can be seen from Fig. S2, B p and N p induce magnetic moments by Co atoms, and the energy range occupied by their PDOS is consistent with that of Co d. This shows that there is a strong interaction between Co d and the p electrons of B and N. Co d, N p and B p states occupies the main role.

S3. Charge density differences of structure

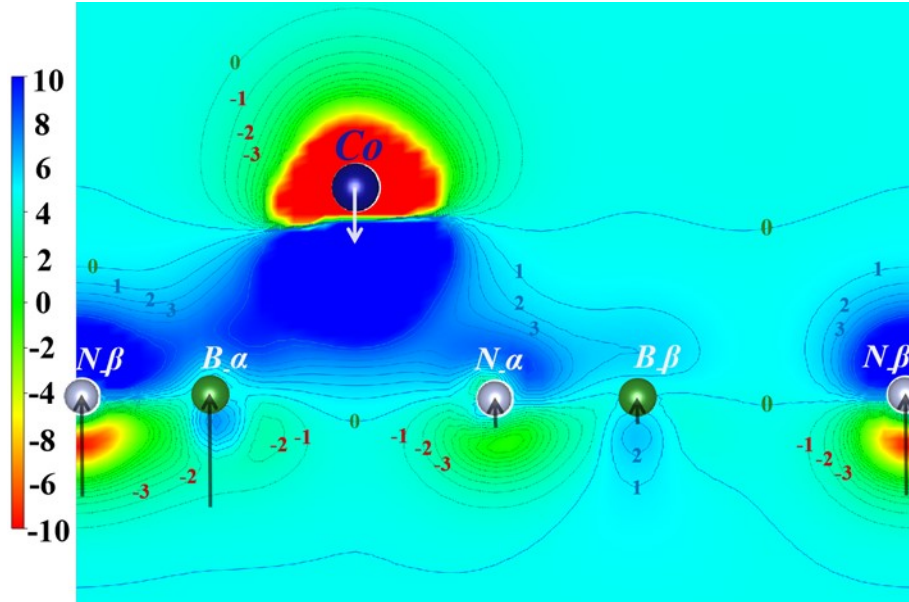


Fig. S3 (Color online) Charge density differences between -0.5 and 0 $\text{eV}/\text{\AA}$ across Co, B and N atoms in the supercell and perpendicular to the film. The contour value is $\rho_n = 0.001 \times n \text{ e}/a_0^3$, where n is the marker value of the medium-high line in the graph, and a_0 is the Bohr radius. The length of the arrow is proportional to the moving distance each atom after in the electric field of -0.5 $\text{eV}/\text{\AA}$. The Co atom drops by 0.15 \AA . The length of the arrow is in centimeters, and the falling distance of the Co atom is doubled by the proportional length. The arrows of N_β, B_α, N_α, and B_β are magnified 100 times.

To illustrate the effect of the electric field on the interaction between the Co adatom and h-BN layer, we calculated the charge density difference without and with a electric field of -0.5 $\text{eV}/\text{\AA}$, as shown in the Fig. S3. It is clear that electron charge accumulates between the Co and h-BN layer, while the electron charge in the outside regions near both the Co and h-BN layer is drained. Therefore, the charge density between the Co adatom and h-BN layer is enhanced with downward electric field, and hence the interaction between them

should be enhanced. This will be essential to generate the DMI.

S4. Magnetic anisotropy energy

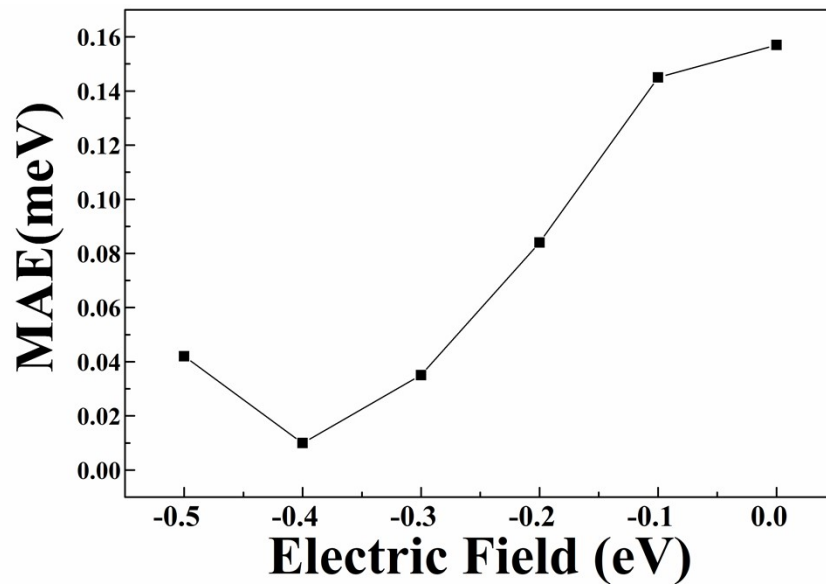


Fig. S4 (Color online) Magnetic anisotropy energy (MAE) of Co/h-BN under the applied variation of the electric field. $MAE = E_{100} - E_{001}$. If the energy of MAE above zero, the easy axis is along with the z axis.

With the increase of the electric field, the value of magnetocrystalline anisotropy energy (MAE) increases as shown in Fig.S3. The easy axis along with z axis and does not change with electric field.

S5. Phonon calculation

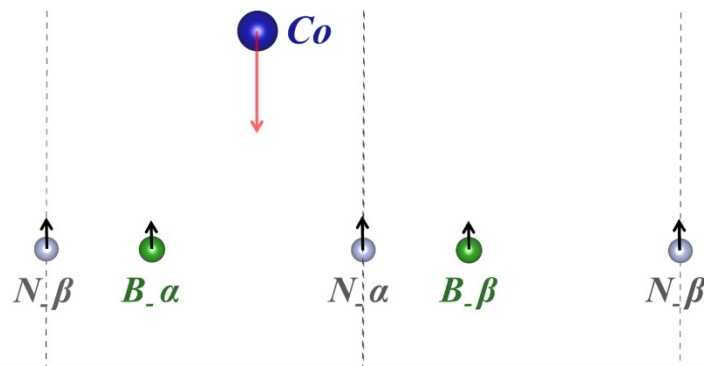
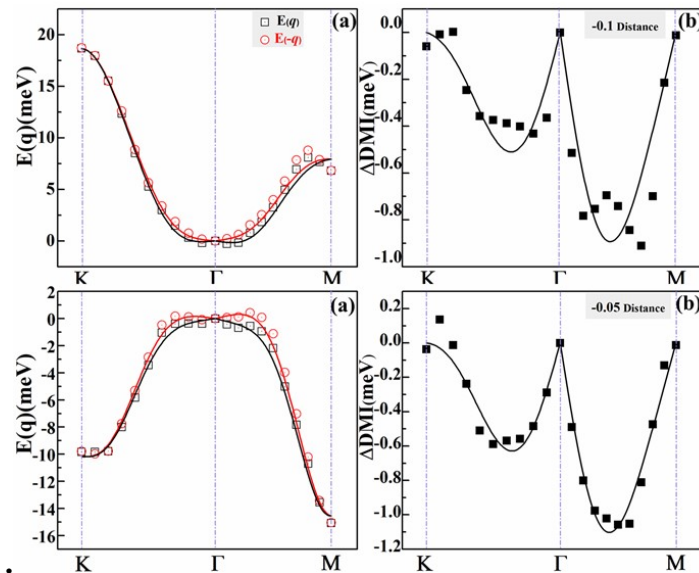


Fig. S5 (Color online) One kind of calculated phonons with the vibration direction along z axis. In this mode, Co and BN layer move towards or away from each other, which is a kind of optical phonon.



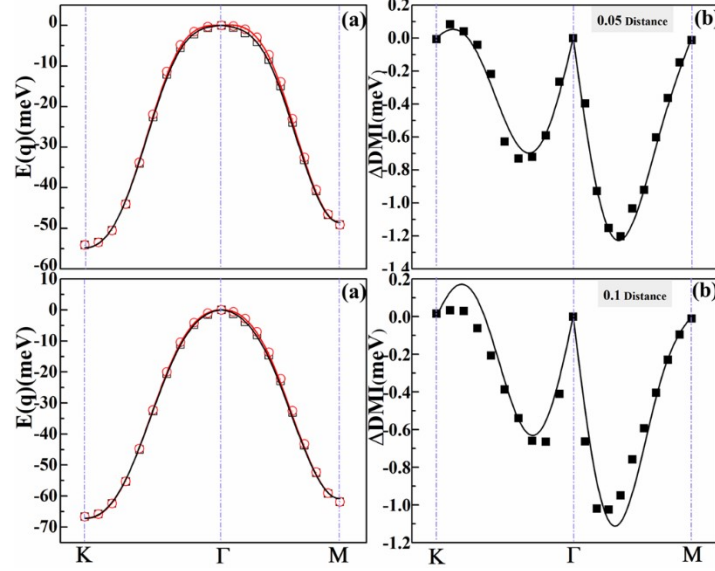


Fig. S5 (Color online) (a) The scattered symbols are calculated energy dispersion $E(q)$ of spin spirals in Co/h-BN as a function of the spiral wave vector q with electric field $-0.5\text{eV}/\text{\AA}$ and the adopted Co at different atomic sites. (b) The scattered symbols are $\Delta\text{DMI}(q)$, gotten from the energy differences between $E(q)$ and $E(-q)$. In (a) and (b), lines are fitted one.

Table 1 Calculated exchanged parameters J_i and d_i with phonon for Co/h-BN in E fields of $-0.5\text{V}/\text{\AA}$

	(meV)					
Structure	J_1	J_2	J_3	J_4	d_1	d_2
-0.1	3.726	-1.511	0.651	-0.117	-0.257	-0.058
-0.05	-3.322	-0.045	1.327	-0.135	-0.309	-0.081
0	-9.470	1.177	1.598	0.036	-0.320	-0.102
+0.05	-13.916	1.342	1.309	0.212	-0.287	-0.153
+0.1	-16.259	0.763	1.042	0.142	-0.198	-0.198

Here, we compare the results with one chosen phonon. It is seen from Fig. S5 and Table

S1 that, although J varies obviously with the phonon, the DMI does not vary much with phonon.

Table 2 Optimized Structural properties for the Co adsorbed on the h-BN at different sites. Bond_{B-Co} and Bond_{N-Co} represents the distance between the Co atom and its nearest B atom(s) (N atom(s)), respectively. h_{Co-BN} is the hight of the Co over the h-BN layer. The rows in bold refer to the most structures.

Site	$\text{Bond}_{B-Co}(\text{\AA})$	$\text{Bond}_{N-Co}(\text{\AA})$	$h_{Co-BN}(\text{\AA})$
tN	2.71	2.26	2.30
tB	2.16	2.66	2.22
b	2.20	2.20	2.13
h	2.39	2.41	1.92

At the tN site, the nearest B-Co and N-Co bond lengths are 2.71 and 2.26 \AA , respectively.

At the tB site, the two bond lengths are 2.66 and 2.22 \AA , At the b site,,the two bond lengths are 2.20 and 2.20 \AA . At the h site, the Co atom locates right above the center of the BN hexagonal ring at the height of 1.92 \AA , the other two bond lengths are 2.39 and 2.41 \AA .

It is worth noting that, the height between Co and h-BN is 2.12 \AA with HSE calculation, which is 0.2 \AA larger than that of 1.92 \AA with no HSE calculation. Under the action of the electric field, this height did not decrease either. Such a long height indicates that the interaction between Co and h-BN will intensify and weaken, especially DMI.

Table 3 Optimized stable structural properties for the Co adsorbed on the h-BN at a hollow sites with different supercells. Tot M denotes the total magnetic moment per unit cell. The last line is the result from reference 22 in the main article.

	Bond _{B-Co} (Å)	Bond _{N-Co} (Å)	h _{Co-BN} (Å)	Tot M(μ_B)
h(2×2)	2.39	2.41	1.92	2.08
h(3×3)	2.37	2.38	1.88	3
h(4×4)	2.37	2.36	1.86	3
Ma ²² (4×4)	2.35	2.37	1.85	3

In table 3, we report the calculated stable structural parameters at a hollow site. Our calculations are consistent with previous calculations.

S6. Additional formulae

With Generalized Bloch Conditions, the magnetic moment $S(\mathbf{R}_j)$ at jth-neighbor with wave vector \mathbf{q} is:

$$\begin{aligned} S(\mathbf{R}_j) &= S(0)\sin(\mathbf{q} \cdot \mathbf{R}_j)\mathbf{i} + S(0)\cos(\mathbf{q} \cdot \mathbf{R}_j)\mathbf{j} \\ &= S(0)\sin 2\pi(mq_1 + nq_2)\mathbf{i} + S(0)\cos 2\pi(mq_1 + nq_2)\mathbf{j} \end{aligned}$$

Then based on Eq. (1), the sum of HBI between $S(0)$ and $S(\mathbf{R}_j)$ is list below respectively:

$$E_{J_1}(\mathbf{q}) = \frac{1}{2}J_1[6 - 2\cos 2\pi q_1 - 2\cos 2\pi(q_1 + q_2) - 2\cos 2\pi q_2]$$

$$E_{J_2}(\mathbf{q}) = \frac{1}{2} J_2 [6 - 2 \cos 2\pi(q_1 + 2q_2) - 2 \cos 2\pi(2q_1 + q_2) - 2 \cos 2\pi(q_1 - q_2)]$$

$$E_{J_3}(\mathbf{q}) = \frac{1}{2} J_3 [6 - 2 \cos 4\pi q_1 - 2 \cos 4\pi(q_1 + q_2) - 2 \cos 4\pi q_2]$$

$$E_{J_4}(\mathbf{q}) = \frac{1}{2} J_4 [12 - 2 \cos 2\pi(2q_1 + 3q_2) - 2 \cos 2\pi(q_1 + 3q_2) - 2 \cos 2\pi(3q_1 + 2q_2) \\ - 2 \cos 2\pi(q_1 - 2q_2) - 2 \cos 2\pi(3q_1 + q_2) - 2 \cos 2\pi(2q_1 - q_2)]$$

Then, the total HBI is

$$E_{HBI}(\mathbf{q}) = E_{J_1}(\mathbf{q}) + E_{J_2}(\mathbf{q}) + E_{J_3}(\mathbf{q}) + E_{J_4}(\mathbf{q})$$

Where, J_1 to J_4 are HBI parameters, including $S(0)^2$.

The sum of DMI between $S(0)$ and $S(R_j)$ is:

$$E_{d_1}(\mathbf{q}) = \frac{1}{2} d_1 [2 \sin 2\pi q_1 + \sin 2\pi(q_1 + q_2) - \sin 2\pi q_2]$$

$$E_{d_2}(\mathbf{q}) = \frac{\sqrt{3}}{2} S^2 d_2 [\sin 2\pi(2q_1 + q_2) + \sin 2\pi(q_1 - q_2)]$$

Where d_1 and d_2 are DMI parameters, including $S(0)^2$, then

$$E_{DMI}(\mathbf{q}) = E_{d_1}(\mathbf{q}) + E_{d_2}(\mathbf{q})$$

The total energy of spin spiral $\mathbf{E}(\mathbf{q})$ contains both HBI and DMI

$$E(\mathbf{q}) = E_{HBI}(\mathbf{q}) + E_{DMI}(\mathbf{q}) \quad (2)$$

Obviously, $\mathbf{E}_{HBI}(\mathbf{q})$ is an even function of \mathbf{q} , while $\mathbf{E}_{DMI}(\mathbf{q})$ is an odd function of \mathbf{q} . Hence,

$$\Delta DMI(\mathbf{q}) = E(\mathbf{q}) - E(-\mathbf{q}) = 2E_{DMI}(\mathbf{q}) \quad (3)$$

S7. Crystal Orbital Hamilton Population (COHP) Analysis

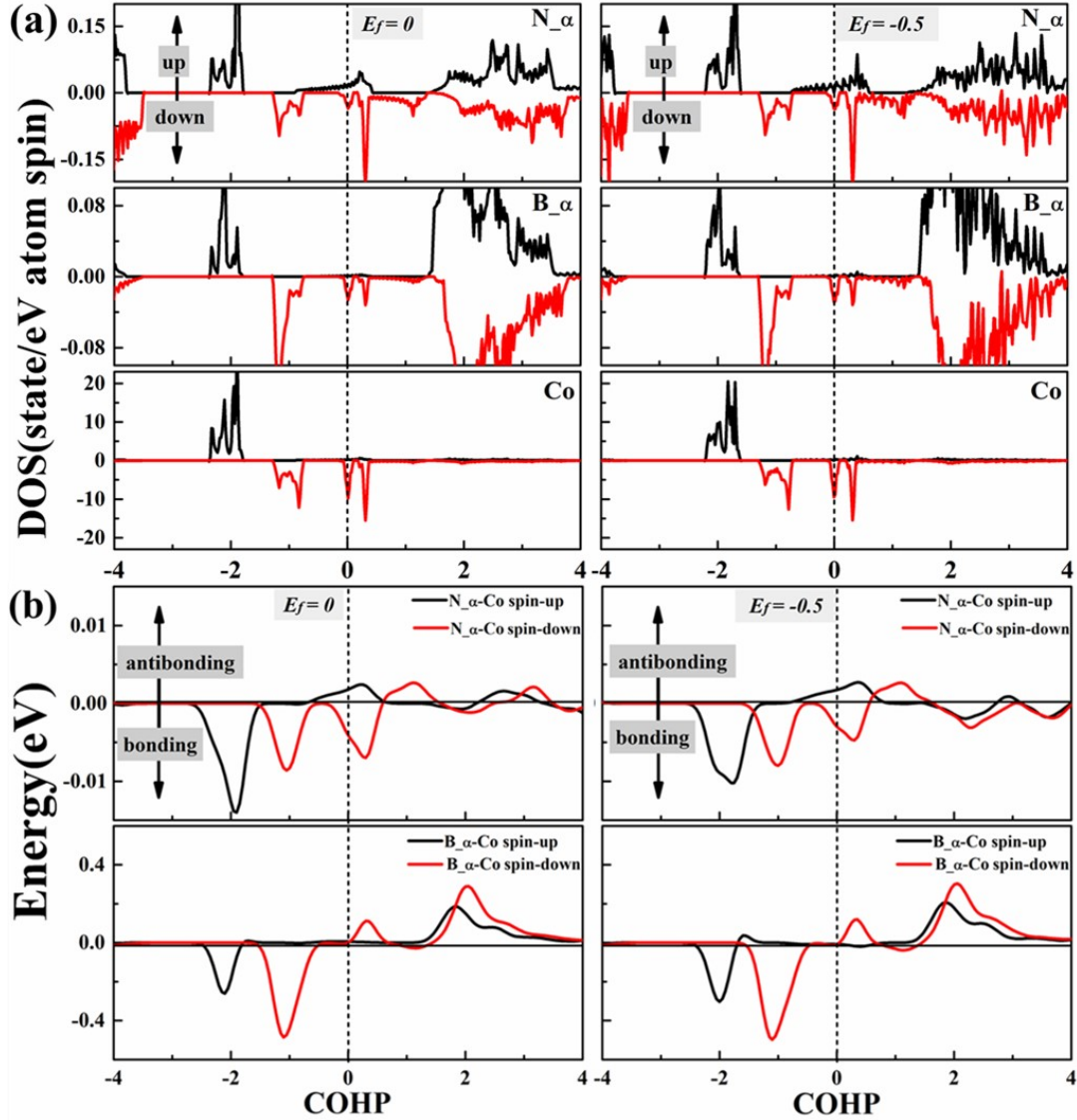


Fig. S7 (Color online) (a) PDOS of B, N (nearest neighbor and next nearest neighbor to Co) and Co atoms in the electric field of -0.5 eV/Å and 0 eV/Å with spin polarization. (b) COHP of B-Co and N-Co bonds in the Co/h-BN system. The black and red line indicates that the spin is up and down, respectively. If $\text{COHP} > 0 (< 0)$, two atoms hybridize in this energy region form an antibonding orbital

(bonding orbital). The Fermi level is denoted by a dashed line at 0 eV.

An analysis of chemical bonding was undertaken using the crystal orbital Hamilton population (COHP) of the metal-adsorbate interactions.^{1,2,3} The analysis was performed using the program LOBSTER⁴. PDOS and COHP curves were drawn to explain the opposite values of binding energy with different spin-polarization conditions, as shown in Fig. S7. PDOS curves will be used to illustrate the orbital interaction and COHP curves will be used to characterize the system stability. In the COHP curve of Fig. S7(b), it is clear that the bonding contribution near Fermi level for the spin down and the spin up significantly contributes to the bonding portion to the N_α-Co bond. We can confirm that Co/h-BN possess bonding-state characters.

1 R. Dronskowski and P. E. Bloechl, *J. Phys. Chem.*, 1993, **97**,8617–8624

2 V. L. Deringer, A. L. Tchougréeff, R. Dronskowski, *J. Phys. Chem. A*., 2011, **115**, 5461.

3 S. Maintz, V. L. Deringer, A. L. Tchougréeff, and R. Dronskowski, *J. Comput. Chem.*, 2013, **34**, 2557

4 S. Maintz, V. L. Deringer, A. L. Tchougréeff, and R. Dronskowski, *J. Comput. Chem.*, 2016, **37**, 1030.